

Chemical Science

Accepted Manuscript



This is an *Accepted Manuscript*, which has been through the Royal Society of Chemistry peer review process and has been accepted for publication.

Accepted Manuscripts are published online shortly after acceptance, before technical editing, formatting and proof reading. Using this free service, authors can make their results available to the community, in citable form, before we publish the edited article. We will replace this *Accepted Manuscript* with the edited and formatted *Advance Article* as soon as it is available.

You can find more information about *Accepted Manuscripts* in the [Information for Authors](#).

Please note that technical editing may introduce minor changes to the text and/or graphics, which may alter content. The journal's standard [Terms & Conditions](#) and the [Ethical guidelines](#) still apply. In no event shall the Royal Society of Chemistry be held responsible for any errors or omissions in this *Accepted Manuscript* or any consequences arising from the use of any information it contains.

Transition Voltages Respond to Synthetic Reorientation of Embedded Dipoles in Self-Assembled Monolayers

Andrii Kovalchuk,[†] Tarek Abu-Husein,[‡] Davide Fracasso,[†] David A. Egger,^{¶,§}
Egbert Zojer,[¶] Michael Zharnikov,^{||} Andreas Terfort,[‡] and Ryan C. Chiechi^{*,†}

[†]*Stratingh Institute for Chemistry & Zernike Institute for Advanced Materials, University of Groningen, Nijenborgh 4, 9747 AG Groningen, The Netherlands*

[‡]*Institut für Anorganische und Analytische Chemie, Universität Frankfurt, Max-von-Laue-Straße 7, 60438 Frankfurt, Germany*

[¶]*Institute of Solid State Physics, NAWI Graz, Graz University of Technology, Graz, Austria*

[§]*Department of Materials and Interfaces, Weizmann Institute of Science, Rehovoth 76100, Israel*

^{||}*Angewandte Physikalische Chemie, Universität Heidelberg, Im Neuenheimer Feld 253, 69120 Heidelberg, Germany*

E-mail: r.c.chiechi@rug.nl

Keywords: EGaIn, dipoles, molecular electronics, self-assembled monolayer, transition voltage, tunneling junction

Abstract

We studied the influence of embedded dipole moments in self-assembled monolayers (SAMs) formed on template stripped Au surfaces with liquid eutectic Ga-In alloy as a top electrode. We designed three molecules based on a *p*-terphenyl structure in which the central aromatic ring is either phenyl or a dipole-inducing pyrimidyl in one of two different orientations. All three form well defined SAMs with similar thickness, packing density and tilt angle, with dipole moments embedded in the SAM, isolated from either interface. The magnitude of current density is dominated by the tunneling distance and is not affected by the presence of dipole moments; however, transition voltages (V_T) show a clear linear correlation with the shift in the work function of Au induced by the collective action of the embedded dipoles. This observation demonstrates that V_T can be manipulated synthetically, without altering either the interfaces or electrodes and that trends in V_T can be related to experimental observables on the SAMs before installing the top contact.

Calculated projected density of states of the SAMs on Au surfaces that relate HOMO-derived states to V_T further show that energy level alignment within an assembled junction can be predicted and adjusted by embedding dipoles in a SAM without altering any other properties of the junction. We therefore suggest that trends in V_T can be used analogously to β in systems for which length-dependence is physically or experimentally inaccessible.

1 Introduction

The field of molecular electronics aims to investigate and realize electronic devices with functionality defined by molecular properties. Two main approaches are currently used to contact molecules, which is a key step in the examination of charge transport: single-molecule and large-area (*i.e.*, ensembles) measurements. In both cases the molecules under investigation are placed in between two metal electrodes that are on the order of 2 nm apart (the exact distance is defined by the dimensions of the molecules under investigation). In

these systems interfaces play an important role in defining the characteristics of a junction and both approaches suffer from an uncertainty—is transport dominated by molecules or by interfaces?^[1,2] Electron transport in large-area junctions is affected by defects in self-assembled monolayers (SAMs) that can dominate transport in certain cases,^[3] while single-molecule junctions exhibit background currents in which tunneling charges flow directly from one electrode to the other, by-passing the molecule in between.^[4] Thus, the magnitude of J or I (current-density or current) by itself varies considerably and therefore carries little useful information on the intrinsic electronic properties of the molecules in the junction.

One of the most reliable metrics that seeks to resolve these issues is β , which is an empirical parameter derived from a form of the Simmons equation $J = J_0 e^{-\beta d}$, where J is the current density, d is the tunneling distance defined by the length of the molecular backbone and J_0 is the theoretical value of J at $d = 0$. Values of β are derived from measurements of series of molecules that differ only by length, while both top and bottom interfaces are kept constant, thus isolating the molecular component in charge transport.^[5,6] This approach to data analysis is particularly robust when comparing saturated molecules (*i.e.*, where the backbone comprises mostly sp^3 -hybridized C atoms), for which the consensus value of β is $\sim 0.75 \text{ \AA}^{-1}$.^[6] Saturated molecules have frontier orbitals that are typically not accessible in the typical bias windows used in molecular electronics and they are not very polarizable. With the exception of end groups that introduce accessible gap states^[7] these properties tend to make saturated molecules less sensitive to the details of the contacts, in general; *e.g.*, tail-groups,^[8–10] anchoring groups,^[11,12] and minor alterations to the backbone^[13] have little impact on the tunneling transport in terms of the magnitudes of I or J . Unsaturation, by contrast, adds significant complexity and even subtle changes in conjugation patterns can have pronounced and non-distance dependent effects on transport.^[14–18] Tuning the length of fully conjugated molecules is also synthetically challenging and not always possible, since a minimal step size is a π bond (*i.e.*, two carbons) or aromatic ring (usually phenylene) and, unlike alkanes, conjugated molecules become markedly less soluble with increasing length.^[19]

Thus, a parameter other than β , but that is comparably independent from non-molecular variables (*e.g.*, interfaces), could greatly assist in the description of tunneling transport phenomena in conjugated molecules and, importantly, in the deconvolution of molecular properties from those of the experimental platform.

Beebe *et al.*^[20] introduced the transition voltage (V_T) as an approximate measure of the tunneling barrier height, which was later related to level alignment—*i.e.*, the difference between the energy of the accessible frontier orbital of a molecule and the Fermi level of the electrode (*e.g.*, $E_{LUMO} - E_F$ or $E_F - E_{HOMO}$) in an assembled junction. The parameter V_T can be extracted from the minimum of a Fowler-Nordheim plot, $\ln(I/V^2)$ versus $1/V$. The possibility of determining the level alignment of a junction by simply re-plotting conductance data has led to a number of experimental^[21–28] and theoretical studies.^[29–33]

While β provides information about the effective tunneling distance (and barrier height), V_T provides information about energy level alignment. Multiple experiments showed a correlation between V_T and apparent energetic separation between the Fermi energy level (E_F) and the dominant frontier molecular orbital.^[34,35] However, the precise physical meaning of V_T is still under debate; *e.g.*, current becomes “superquadratic” with bias and might not always correlate to energy spectral transition.^[30,36] Sotthewes *et al.*,^[37] studied vacuum gaps in ultra-high vacuum STM junctions and found that transition voltage is inversely proportional to $1/d$; *i.e.*, that work showed that V_T can even be measured in the absence of molecules.

Summarizing the above considerations, we assert that the interpretation of V_T is not straightforward and that V_T is highly dependent on interfaces and is a conflation of two effects—interfacial and molecular—underscoring the importance of separating one from the other. This paper describes the control over V_T by manipulating a single parameter—embedded dipoles—while keeping the interfaces and electrodes constant, allowing the unambiguous assignment of *trends* in V_T and energy level alignment to an intrinsic molecular property.

2 Results and discussion

J/V Measurements. We investigated the influence of embedded dipoles on electron transport of SAMs placing them in EGaIn junctions of the form $\text{Au}^{\text{TS}}/\text{SAM}/\text{Ga}_n\text{O}_m/\text{EGaIn}$ (where “/” denotes an interface defined by chemisorption and “//” by physisorption).^[38] Here EGaIn stands for eutectic alloy of Ga and In (75.5% Ga and 24.5% In by weight, mp = 15.7 °C) which is covered by a superficial layer of ~ 0.7 nm of conductive Ga_nO_m . Multiple studies have shown that the oxide layer has a negligible effect on transport properties in EGaIn junctions and is orders of magnitude more conductive than the contacts.^[6,38–40] We designed three structures (depicted and assigned in Fig. 1) for this study that possess identical length, surface chemistry, and nearly identical gas-phase frontier orbital energies; for TP1-down and up they are identical (as is their empirical formula). All three compounds form well-defined SAMs on template-stripped Au (Au^{TS})^[41] and were extensively characterized by a number of complementary surface-analytical techniques,^[42] exhibiting comparable film thickness and packing densities (see Table 1). The discernible difference is the dipole moment associated with the central aromatic ring (either a pyrimidine or benzene).

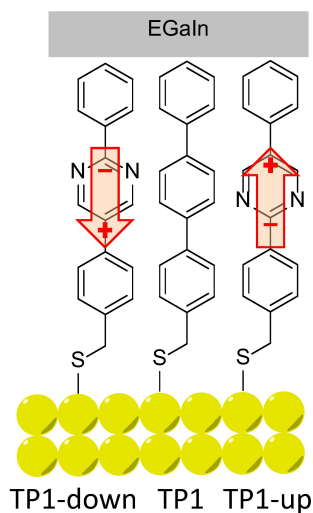


Figure 1: Schematic of a junction with two pyrimidyl-containing compounds (TP1-down and TP1-up) and the reference compound (TP1). Arrows indicate directions of dipole moments associated with the embedded pyrimidine rings (from negative to positive charge).

An immediate consequence of the collective effect of SAMs of polar pyrimidyl groups

is the modification of the electrostatic potential profile, which shifts the vacuum level and the energy separation between E_F and frontier molecular orbitals. Transition voltages offer insight into the effects of electrostatic fields induced by SAMs because they carry information about the level alignment between the frontier molecular orbitals and the Fermi energies of the electrodes. This information is inaccessible experimentally and is challenging to model theoretically, as the details of alignment between molecular and electrode levels are difficult to predict.^[43,44] Our experimental approach is to vary an internal, molecular property—in this case dipole moments—and measure the effect in a SAM supported by a bottom electrode (*i.e.*, *ex situ*) before the top contact is installed. We chose shifts in the work function of the bottom electrode (Φ) because work function shift ($\Delta\Phi$) is defined by the collective effect of embedded dipoles in the SAM.^[45] This collective effect is preserved when the top contact is installed (*i.e.*, *in situ*), because the dipoles are embedded in the SAM and are isolated from both interfaces. After assembling the junction and performing electrical measurements, we extracted V_T and plotted it against $\Delta\Phi$ to give us two experimental parameters, one intrinsic to the SAM/bottom-contact ($\Delta\Phi$) and one to the bottom-contact/SAM//top-contact (V_T). This approach is similar to that of the β analysis, where tunneling distance d (which is an *ex situ* parameter and can be calculated and measured in multiple ways) is correlated to current density J (an *in situ* characteristic of an assembled junction). It is important to compare trends because the absolute magnitude of V_T is still affected by the details of the contacts.^[26,36]

Figure 2 summarizes measurements of tunneling current through SAMs of TP1, TP1-down, and TP1-up. These data were acquired by sweeping the potential in EGaIn junctions through a range of $\pm 1V$. (See Supporting Information for a detailed description of data acquisition and analysis.) As expected, the conductances of all SAMs are nearly identical. The magnitude of current is dominated by the tunneling distance, which is identical along the series, and is influenced only slightly, if at all, by the embedded dipoles ($\beta \approx 0.4 \text{ \AA}^{-1}$ for these backbones^[46]). All of the curves are slightly asymmetric,^[47] with TP1-up showing

Table 1: X-ray photoemission spectroscopy derived effective thickness and packing density of TP1, TP1-up and TP1-down SAMs; X-ray absorption spectroscopy derived tilt angles; WF shifts with respect to pristine gold.

TP1	1.78 ± 0.04	4.6×10^{14}	$18 \pm 3^\circ$	0.98
TP1-up	1.74 ± 0.05	4.2×10^{14}	$18 \pm 3^\circ$	1.41 (+0.43 ^b)
TP1-down	1.75 ± 0.05	4.3×10^{14}	$17 \pm 3^\circ$	0.43 (-0.55 ^b)

Experimental values are from Reference 42.

^a Measured with a Kelvin probe; we use opposite sign conventions for Φ .

^b Difference from TP1.

opposite asymmetry—it conducts slightly more at negative bias as opposed to TP1 and TP1-down, which are slightly less conductive at negative bias (but values of $J(+)$ and $J(-)$ are within error for most values of V for all three SAMs, see the Supporting Information). Though there is evidence that terminal pyrimidine rings can induce asymmetry in J/V traces^[48–50] (which can theoretically be caused by internal dipole moments as well,^[51]) we are hesitant to ascribe the observed asymmetry solely to the presence of molecular dipoles, since TP1 (which does not possess an embedded dipole) and TP1-down exhibit comparable degrees of asymmetry. However we can eliminate packing, tilt, and the molecule-electrode interfaces, as these parameters are effectively identical for the three SAMs. The difference in the symmetry of the J/V curve of TP1-up may be related to the effect of the direction of the dipole moments on the hybridization of the HOMO with states in the gold electrode (see below).

Transition Voltage Measurements. We calculated V_T by re-plotting raw I/V data as $\ln(I/V^2)$ versus $1/V$ for both positive and negative biases for each J/V curve and extrapolating the minimum (see the Supporting Information for details on V_T acquisition). The peak values of Gaussian fits (μ) to the resulting distributions are taken as V_T and the error is derived from the widths (σ). These data are summarized in Table 2 along with gas-phase HOMO energies and dipole moments calculated using structural information from the characterization of the SAMs (as described in reference 46). The HOMO energies serve only to

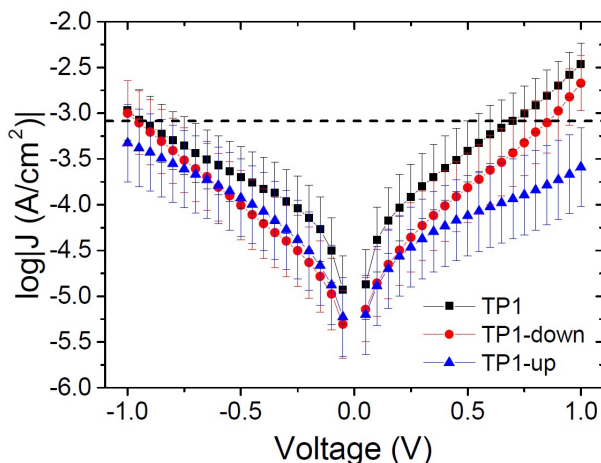


Figure 2: Plots of log current-density versus applied potential for SAMs of TP1 (black squares), TP1-down (red circles) and TP1-up (blue triangles). Values of $\log|J|$ at $V = 0$ are omitted for clarity. Error bars represent 95% confidence intervals. The three traces are hardly distinguishable at negative bias, while, at positive bias, TP1-up deviates from the rest showing opposite asymmetry ($J(+1V)$ is slightly higher than $J(-1V)$ for TP1 and TP1-down and opposite for TP1-up).

highlight the electronic similarities between the three compounds, not the SAMs. The values of V_T at negative bias (denoted V_T^-) are systematically higher than the corresponding values of V_T^+ , which is common for EGaIn junctions,^[26,46] but they follow the same trend; increasing from TP1-down to TP1 to TP1-up. The value of V_T^+ for TP1 is in good agreement with the previously reported value of 0.55 ± 0.10 V.^[46] The general trend is also in agreement; “down” dipole moments lower both V_T^- and V_T^+ with respect to “up” dipole moments.

Table 2: Values of V_T for all SAMs for positive (V_T^+) and negative bias (V_T^-) and gas-phase calculated HOMO energies. Errors are 95% CI.

SAM	V_T^+ (V)	V_T^- (V)	HOMO ^a (eV)	μ_{net}^a (D)
TP1	0.52 ± 0.05	-0.65 ± 0.05	-5.65	+0.01
TP1-up	0.80 ± 0.06	-0.85 ± 0.03	-6.08	-2.75
TP1-down	0.40 ± 0.02	-0.43 ± 0.04	-6.08	+2.34

^a Gas-phase HSE06/6-311+g(2d,2p) DFT calculations.

Level Alignment. As a result of collective effect of individual dipoles, SAMs of TP1-down and TP1-up shift the electrostatic energy within the junction, which alters the relative positions of the frontier orbitals and the Fermi levels of the electrodes leading to a change in

V_T . The magnitude of the shift can be approximated by measuring the work function of the bare Au^{TS} substrate and the substrate supporting a SAM using Kelvin probe measurements or UPS.^[46] Kim *et al.*^[24] demonstrated correlation of V_T versus $\Delta\Phi$ using conducting AFM tips to contact SAMs; however, they adjusted Φ by varying materials of either bottom or top electrodes, not the electronics of the molecules. Another study found a correlation between V_T and interfacial dipoles, but could not unambiguously assign it to a molecular property.^[46] The effects of embedded dipolar groups have also been investigated in aliphatic SAMs (*i.e.*, comprising CH₂ backbones), including a study of the physical and electronic structure effects of embedded esters^[52] as well as a study of the J/V properties of embedded amides,^[9] however, no correlation to V_T has been established. Taking TP1 as a reference point, the shifts in TP1-down and up are $\Delta\Phi = -0.55$ and $+0.43$ eV (see Table 1), respectively; they are shifted by approximately the same amount, but opposite in sign, from TP1. Figure 3 shows plots of V_T^+ and V_T^- versus $\Delta\Phi$. The plots are approximately linear, fitting with $R^2 = 0.77$ and 0.99 respectively, demonstrating that V_T correlates to the shift in vacuum level of Au^{TS} induced by the embedded dipoles of the SAMs. A symmetric offset is apparent for V_T^- , which differs from TP1 by $\sim \pm 0.2$ V, but less so for V_T^+ ; however, the correlation of the latter to $\Delta\Phi$ is also less robust. Thus, it appears that the simple picture in Fig. 1 is a reasonable, qualitative description of the synthetic manipulation of V_T .

DFT Calculations. Valuable insight can be gained from the level alignment of the molecular states relative to the Fermi energy of the Au substrate in the absence of the EGaIn (top) electrode. Thus, we plot the DFT calculated projected densities of states (PDOS) associated with the three studied monolayers in Fig. 4. We used the hybrid functional HSE^[53,54] for the periodic band-structure calculations (performed with the VASP code,^[55] see the Supporting Information for details) for the metal-SAM systems as, due to the mixing of short-range Fock and semi-local exchange, orbital self-interactions errors that would distort the electronic structure of pyrimidyl-containing systems can be reduced.^[56,57] However, the absolute values of the calculated level alignment, especially for

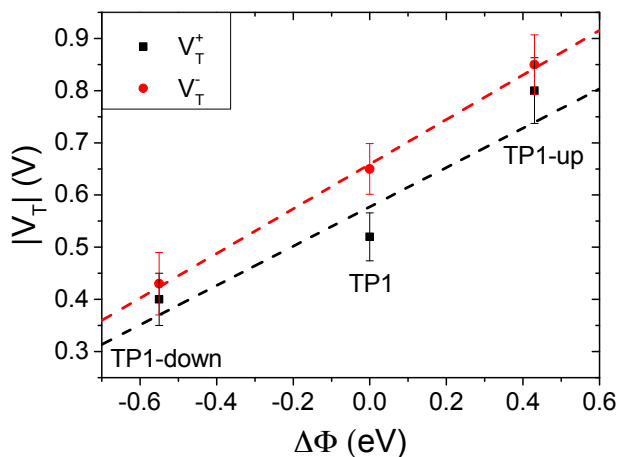


Figure 3: Plot of V_T^+ (black squares, fitting with the slope of 0.38 and $R^2 = 0.77$) and V_T^- (red circles, slope of 0.43 and $R^2 = 0.99$) versus work function shift. Values of $\Delta\Phi$ are taken from Table 1.

upright-standing molecules,^[58] cannot quantitatively reproduce the experiment even with the hybrid-functionals used here.^[43,59,60] Nevertheless, for chemically similar systems such as the ones studied here, advanced hybrid DFT-calculations allow for predicting trends in the level alignment.

In Fig. 4, one clearly sees that in TP1-down the highest occupied states are shifted towards E_F compared to the reference TP1 system, while they are shifted away in the TP1-up case. These shifts can be understood from the peculiar distribution of the electrostatic energy within the SAM where, due to collective electrostatic effects^[61,62] (i.e., the superposition of the fields of the pyrimidyl dipoles arranged in a 2D pattern), the electrostatic energy in the topmost rings is shifted relative to E_F (as schematically shown in Fig. 5, a plot of the calculated plane-averaged potentials can be found in ref. 42). This shift has been confirmed by high-resolution XPS experiments.^[42] And because the occupied frontier states are largely delocalized over the SAM, a shift in the electrostatic energy induces a shift in the SAM eigenstates relative to E_F (see Fig. 5).

The frontier orbitals are largely delocalized over the molecular backbone, likely leading to highly transmissive channels in the transport experiments. Nevertheless, one can see that in the TP1-down (TP1-up) case the HOMO-derived PDOS has a larger weight on the ring

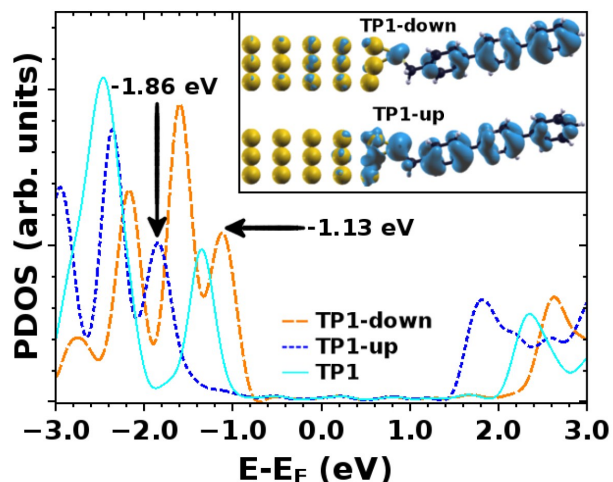


Figure 4: Density of states of TP1, TP1-up and TP1-down projected (PDOS) onto the molecular region as calculated with HSE. The energy scale is given relative to the Fermi-energy, E_F ; inset depicts charge density associated with the highest occupied peaks in the PDOS (derived from the molecular HOMO) of TP1-down (top) and TP1-up (bottom). The latter are calculated per system in a ± 0.1 eV interval centered at the energy indicated by an arrow (isodensity value: $0.01 \text{ e}\text{\AA}^{-3}$)

far from (close to) the Au substrate, which is the behavior expected for such a situation,^[63] as can be understood, for example, from the analogy of SAM-states and electron- and hole-states in quantum-well states in the presence of a potential gradient.^[56] This difference in the spatial distribution of PDOS densities might also be responsible for the qualitative differences in the shapes of the J/V curves for SAMs of TP1-up and TP1-down (Fig. 2).

The question remains as to what exactly happens at V_T , *e.g.*, if the tail of density of states comes into resonance with E_F . A calculation of the PDOS for SAMs bound to a metal surface made by plotting the peaks in Fig. 4 produces good correlation of V_T versus peak values of HOMO levels (Fig. 6). The slopes of linear fits for both V_T^+ and V_T^- are almost equal (0.56 and 0.55 respectively) and in good agreement with the experimentally determined slope of 0.55 reported by Beebe *et al.*^[21] Regardless of the exact physical meaning of the magnitude of V_T , from the trend it is clearly possible to “feel” energy level alignment in these SAMs. Moreover, the agreement in the slopes suggests that shifting the vacuum level by embedding dipoles in a SAM is physically similar to changing the identity of the electrodes, while the effects of dipoles placed at the physisorbed interface are more convoluted.^[46]

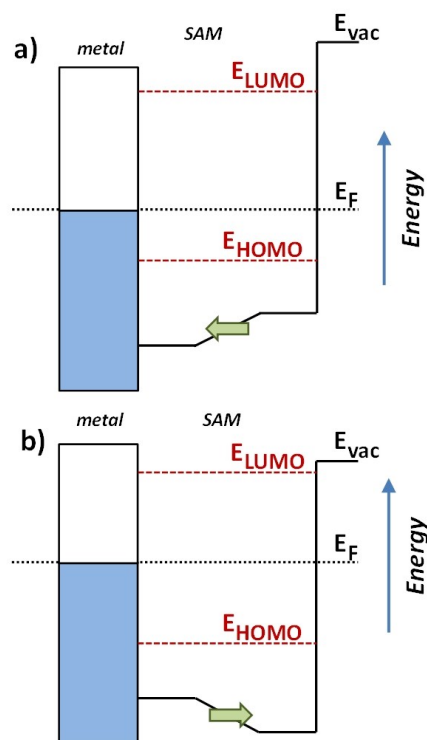


Figure 5: Schematics of the electrostatic energy distribution and the resulting energy-level alignment in TP1-down (a.) and TP1-up (b.) SAMs on Au electrode. The right (upper) parts of the potential well are shifted up, respectively down in energy as a consequence of the pyrimidyl dipoles arranged in a 2D plane. The SAM eigenstates (partially) follow that shift.

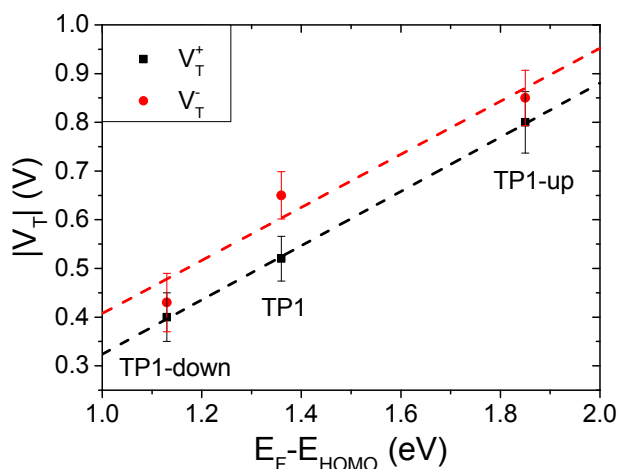


Figure 6: Plot of V_T^+ (black squares, fitting with the slope of 0.56 and $R^2 = 1$) and V_T^- (red circles, slope of 0.55 and $R^2 = 0.87$) vs $E_F - E_{HOMO}$ from the calculated density of states. Error bars are 95% CI.

Trends in Transition Voltages. Just as the absolute value of J for an isolated member of a series of molecules (from which one cannot make a J vs d plot to extract β) is significantly less useful than β , the absolute value of V_T carries complex, inseparable information and is less useful than a trend that relates a shift in V_T to a controllable variable. The trend presented in Fig. 3 shows that a shift in V_T is correlated to a change in Φ (hence dipole moment) revealing a molecular fingerprint in the transport properties. For any series of molecules of equal length β is obviously not applicable, thus trends in V_T might serve as empirical evidence that transport is dominated by tunneling through molecules (Fig. S3). The ability to make this distinction is both important and non-trivial. For example, one can observe quantum interference effects as a length-independent decrease in J with varying conjugation patterns,^[14] a lack of measurable current in *meta* substituted stilbene thiols^[64] or negative curvature in $\log|dI/dV|$,^[16] but these interpretations all rely on the underlying assumption that I and J are dominated by transport through molecules. Likewise, applying theoretical models to explain the interference effects relies on the same assumptions. This problem is particularly evident when experimental observations that disagree with theory are based on a somewhat ambiguous interpretations of data (*i.e.*, bi-modal distributions of conductance).^[65] The series of molecules in this paper is not expected to exhibit any unusual transport properties, but despite the lack of a distance-dependence the J/V data presented in Fig. 2 are unambiguously dominated by transport through molecules. And we have shown that embedded dipoles have a measurable influence on the energetics within molecular tunneling junctions comprising TP1, TP1-down, and TP1-up, but do not have a significant influence on the magnitude of tunneling charge-transport.

Conclusions

We examined tunneling junctions comprising SAMs of three molecules of nearly identical length, packing density, tilt angle, torsional angle and gas-phase HOMO energies.^[42] The only

difference is the inclusion of a central pyrimidine ring, which introduces a dipole moment, the direction of which is synthetically controllable by adjusting the orientation of the ring. The resulting dipole moments are embedded in the SAM as opposed to being introduced as a head (tail) group in contact with the top (bottom) electrode. Thus, we can eliminate both electrode interfaces, tunneling distance, packing, tilt, torsional angles, and gas-phase HOMO energies as variables and compare the tunneling transport properties.

We find that, outside of a slight difference in J at $+1V$, the J/V curves are indistinguishable and this slight difference may be the result of the dipole moments affecting the distribution of HOMO-derived PDOS on or off of the Au electrode. The transition voltages, however, differ systemically and follow the same trend as the experimentally-determined vacuum level shift induced by the direction and magnitude of the embedded dipoles. The trends in Fig. 3 and 6 capture the critical aspect of investigating systematic behavior in V_T . The former relates an external experimental observable, Φ , to an internal experimental observable, V_T . The latter relates this internal observable to the details of the level alignment that takes place when molecules are chemisorbed to a metal, which can in turn be related to experimentally observable energy positions of frontier electronic states.^[24] Thus, the ability to manipulate V_T systematically through synthetic modifications away from the electrode interfaces simultaneously provides evidence that the charge transport is dominated by molecules and provides quantitative information about their electronic states. This physical interpretation of V_T is not new, but the isolation of the internal electrostatic profile of a molecule as a variable that affects V_T is an important step forward in the fundamental understanding of tunneling transport through molecular junctions and, ultimately, control over functionality.

This result demonstrates that (i) V_T can be manipulated synthetically in a predictable manner, (ii) changes to V_T can be ascribed to an intrinsic property of the molecules inside the tunneling junction, (iii) the energy level alignment can be adjusted using embedded dipoles without altering any other characteristic of a SAM. And, while the length dependence of

conductance can be described by β , V_T carries information about energy levels; trends in V_T can separate some of these influences. The inclusion of embedded dipoles (or specifically pyrimidine rings) instills a “molecular fingerprint” to tunneling transport that is separate from the magnitude of I or J . This observation is in agreement with studies showing that polar groups (and embedded dipoles in saturated molecules) have no influence on β .^[9] While the lone pairs of a pyrimidyl moiety can interfere with edge-to- π interactions, in this particular case all three SAMs pack nearly identically.^[42] Thus, this effect is sufficiently weak that it is overcome by the flanking phenyl rings, suggesting that the use of pyrimidine rings specifically to create a dipole moment is generalizable. We suggest that, irrespective of the precise physical interpretation of transition voltages, trends in V_T —specifically V_T versus $\Delta\Phi$ —are particularly useful for unsaturated molecules in which molecular length is synthetically or experimentally inaccessible or in cases where β is not sensitive to synthetic alterations.

Acknowledgement

RCC, DF, and AK acknowledge the European Research Council for the ERC Starting Grant 335473 (MOLECSYNCON). TW and MZ thank the Max-IV staff, and A. Preobrajenski in particular, for the technical support during the experiments at the synchrotron. Part of this work was supported financially by the Deutsche Forschungsgemeinschaft (grants ZH 63/14-2). DAE and EZ acknowledge financial support by the Austrian Science Fund (FWF): project I937-N19 within the ERAChemistry framework and project P24666-N20. The computational studies presented have been mainly performed using the clusters of the division for high-performance computing at the Graz University of Technology.

References

- (1) L. A. Bumm, *ACS Nano* **2008**, *2*, 403–407.
- (2) S. L. Bernasek, *Angew. Chem. Int. Ed.* **2012**, *51*, 9737–9738.
- (3) L. Jiang, C. S. S. Sangeeth, A. Wan, A. Vilan, C. A. Nijhuis, *J. Phys. Chem. C* **2015**, *119*, 960–969.
- (4) B. Gotsmann, H. Riel, E. Lörtscher, *Phys. Rev. B* **2011**, *84*, 205408.
- (5) E. A. Weiss, R. C. Chiechi, G. K. Kaufman, J. K. Kriebel, Z. Li, M. Duati, M. A. Rampi, G. M. Whitesides, *J. Am. Chem. Soc.* **2007**, *129*, 4336–4349.
- (6) F. C. Simeone, H. J. Yoon, M. M. Thuo, J. R. Barber, B. Smith, G. M. Whitesides, *J. Am. Chem. Soc.* **2013**, *135*, 18131–18144.
- (7) C. A. Nijhuis, W. F. Reus, J. R. Barber, M. D. Dickey, G. M. Whitesides, *Nano Lett.* **2010**, *10*, 3611–3619.
- (8) H. J. H. Yoon, N. D. N. Shapiro, K. M. K. Park, M. M. M. Thuo, S. S. Soh, G. M. G. Whitesides, *Angew. Chem. Int. Ed.* **2012**, *51*, 4658–4661.
- (9) H. J. Yoon, C. M. Bowers, M. Baghbanzadeh, G. M. Whitesides, *J. Am. Chem. Soc.* **2014**, *136*, 16–19.
- (10) F. Mirjani, J. M. Thijssen, G. M. Whitesides, M. A. Ratner, *ACS Nano* **2014**, *8*, 12428–12436.
- (11) K. C. Liao, H. J. Yoon, C. M. Bowers, F. C. Simeone, G. M. Whitesides, *Angew. Chem. Int. Ed.* **2014**, *53*, 3889–3893.
- (12) D. Fracasso, S. Kumar, P. Rudolf, R. C. Chiechi, *RSC Adv.* **2014**, *4*, 56026–56030.

- (13) M. M. Thuo, W. F. Reus, F. C. Simeone, C. Kim, M. D. Schulz, H. J. Yoon, G. M. Whitesides, *J. Am. Chem. Soc.* **2012**, *134*, 10876–10884.
- (14) D. Fracasso, H. Valkenier, J. C. Hummelen, G. C. Solomon, R. C. Chiechi, *J. Am. Chem. Soc.* **2011**, *133*, 9556–9563.
- (15) N. Gorczak, N. Renaud, S. Tarkuç, A. J. Houtepen, R. Eelkema, L. D. A. Siebbeles, F. C. Grozema, *Chem. Sci.* **2015**, *6*, 4196–4206.
- (16) C. M. Guédon, H. Valkenier, T. Markussen, K. S. Thygesen, J. C. Hummelen, S. J. van der Molen, *Nature Nanotech.* **2012**, *7*, 305–309.
- (17) C. R. Arroyo, S. Tarkuc, R. Frisenda, J. S. Seldenthuis, C. H. M. Woerde, R. Eelkema, F. C. Grozema, H. S. J. vanderZant, *Angew. Chem. Int. Ed.* **2013**, *52*, 3152–3155.
- (18) H. Valkenier, C. M. Guédon, T. Markussen, K. S. Thygesen, S. J. van der Molen, J. C. Hummelen, *Phys. Chem. Chem. Phys.* **2014**, *16*, 653–662.
- (19) Q. Lu, K. Liu, H. Zhang, Z. Du, X. Wang, F. Wang, *ACS Nano* **2009**, *3*, 3861–3868.
- (20) J. M. Beebe, B. Kim, J. W. Gadzuk, C. Daniel Frisbie, J. G. Kushmerick, *Phys. Rev. Lett.* **2006**, *97*, 026801.
- (21) J. M. Beebe, B. Kim, C. D. Frisbie, J. G. Kushmerick, *ACS Nano* **2008**, *2*, 827–832.
- (22) N. Bennett, G. Xu, L. J. Esdaile, H. L. Anderson, J. E. Macdonald, M. Elliott, *Small* **2010**, *6*, 2604–2611.
- (23) S. Guo, J. Hihath, I. Díez-Pérez, N. Tao, *J. Am. Chem. Soc.* **2011**, *133*, 19189–19197.
- (24) B. Kim, S. H. Choi, X.-Y. Zhu, C. D. Frisbie, *J. Am. Chem. Soc.* **2011**, *133*, 19864–19877.
- (25) M. C. Lennartz, N. Atodiresei, V. Caciuc, S. Karthäuser, *J. Phys. Chem. C* **2011**, *115*, 15025–15030.

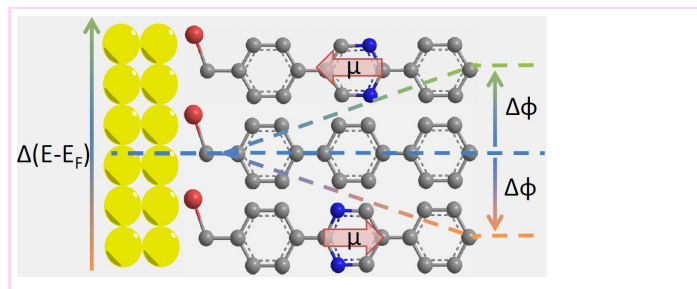
- (26) G. Ricœur, S. Lenfant, D. Guérin, D. Vuillaume, *J. Phys. Chem. C* **2012**, *116*, 20722–20730.
- (27) X. Lefèvre, F. Moggia, O. Segut, Y.-P. Lin, Y. Ksari, G. Delafosse, K. Smaali, D. Guérin, V. Derycke, D. Vuillaume, S. Lenfant, L. Patrone, B. Joussetme, *J. Phys. Chem. C* **2015**, *119*, 5703–5713.
- (28) S. Guo, G. Zhou, N. Tao, *Nano Lett.* **2013**, *13*, 4326–4332.
- (29) I. Bâldea, *J. Am. Chem. Soc.* **2012**, *134*, 7958–7962.
- (30) M. Araidai, M. Tsukada, *Phys. Rev. B* **2010**, *81*, 235114.
- (31) E. H. Huisman, C. M. Guédon, B. J. van Wees, S. J. van der Molen, *Nano Lett.* **2009**, *9*, 3909–3913.
- (32) J. Chen, T. Markussen, K. S. Thygesen, *Phys. Rev. B* **2010**, *82*, 121412.
- (33) I. Bâldea, *Phys. Rev. B* **2012**, *85*, 035442.
- (34) A. Tan, J. Balachandran, B. D. Dunietz, S.-Y. Jang, V. Gavini, P. Reddy, *Appl. Phys. Lett.* **2012**, *101*, 243107.
- (35) G. Wang, Y. Kim, S.-I. Na, Y. H. Kahng, J. Ku, S. Park, Y. H. Jang, D.-Y. Kim, T. Lee, *J. Phys. Chem. C* **2011**, *115*, 17979–17985.
- (36) A. Vilan, D. Cahen, E. Kraissler, *ACS Nano* **2013**, *7*, 695–706.
- (37) K. Sotthewes, C. Hellenthal, A. Kumar, H. J. W. Zandvliet, *RSC Adv.* **2014**, *4*, 32438–32442.
- (38) R. C. Chiechi, E. A. Weiss, M. D. Dickey, G. M. Whitesides, *Angew. Chem. Int. Ed.* **2008**, *120*, 148–150.

- (39) W. F. Reus, M. M. Thuo, N. D. Shapiro, C. A. Nijhuis, G. M. Whitesides, *ACS Nano* **2012**, *6*, 4806–4822.
- (40) C. A. Nijhuis, W. F. Reus, J. R. Barber, G. M. Whitesides, *J. Phys. Chem. C* **2012**, *116*, 14139–14150.
- (41) E. A. Weiss, G. K. Kaufman, J. K. Kriebel, Z. Li, R. Schalek, G. M. Whitesides, *Langmuir* **2007**, *23*, 9686–9694.
- (42) T. Abu-Husein, S. Schuster, D. A. Egger, M. Kind, T. Santowski, A. Wiesner, R. Chiechi, E. Zojer, A. Terfort, M. Zharnikov, *Adv. Func. Mater.* **2015**, *25*, 3943–3957.
- (43) J. B. Neaton, M. S. Hybertsen, S. G. Louie, *Phys. Rev. Lett.* **2006**, *97*, 216405.
- (44) S. Y. Quek, L. Venkataraman, H. J. Choi, S. G. Louie, M. S. Hybertsen, J. B. Neaton, *Nano Lett.* **2007**, *7*, 3477–3482.
- (45) D. M. Alloway, M. Hofmann, D. L. Smith, N. E. Gruhn, A. L. Graham, R. Colorado, V. H. Wysocki, T. R. Lee, P. A. Lee, N. R. Armstrong, *J. Phys. Chem. B* **2003**, *107*, 11690–11699.
- (46) D. Fracasso, M. I. Muglali, M. Rohwerder, A. Terfort, R. C. Chiechi, *J. Phys. Chem. C* **2013**, *117*, 11367–11376.
- (47) H. J. Yoon, K. C. Liao, M. R. Lockett, S. W. Kwok, M. Baghbanzadeh, G. M. Whitesides, *J. Am. Chem. Soc.* **2014**, *136*, 17155–17162.
- (48) G. M. Morales, P. Jiang, S. Yuan, Y. Lee, A. Sanchez, W. You, L. Yu, *J. Am. Chem. Soc.* **2005**, *127*, 10456–10457.
- (49) Y. Lee, B. Carsten, L. Yu, *Langmuir* **2009**, *25*, 1495–1499.

- (50) I. Díez-Pérez, J. Hihath, Y. Lee, L. Yu, L. Adamska, M. A. Kozhushner, I. I. Oleynik, N. Tao, *Nature Chem.* **2009**, *1*, 635–641.
- (51) G. Zhang, M. A. Ratner, M. G. Reuter, *J. Phys. Chem. C* **2015**, *119*, 6254–6260.
- (52) O. M. Cabarcos, A. Shaporenko, T. Weidner, S. Uppili, L. S. Dake, M. Zharnikov, D. L. Allara, *J. Phys. Chem. C* **2008**, *112*, 10842–10854.
- (53) J. Heyd, G. E. Scuseria, M. Ernzerhof, *J. Chem. Phys.* **2003**, *118*, 8207–8215.
- (54) J. Heyd, G. E. Scuseria, M. Ernzerhof, *J. Chem. Phys.* **2006**, *124*, 219906.
- (55) G. Kresse, J. Furthmüller, *Phys. Rev. B* **1996**, *54*, 11169–11186.
- (56) F. Rissner, D. A. Egger, A. Natan, T. Körzdörfer, S. Kümmel, L. Kronik, E. Zojer, *J. Am. Chem. Soc.* **2011**, *133*, 18634–18645.
- (57) N. Dori, M. Menon, L. Kilian, M. Sokolowski, L. Kronik, E. Umbach, *Phys. Rev. B* **2006**, *73*, 195208.
- (58) A. M. Track, F. Rissner, G. Heimel, L. Romaner, D. Käfer, A. Bashir, G. M. Rangger, O. T. Hofmann, T. Bučko, G. Witte, E. Zojer, *J. Phys. Chem. C* **2010**, *114*, 2677–2684.
- (59) A. Biller, I. Tamblyn, J. B. Neaton, L. Kronik, *J. Chem. Phys.* **2011**, *135*, 164706.
- (60) D. A. Egger, Z.-F. Liu, J. B. Neaton, L. Kronik, *Nano Lett.* **2015**, *15*, 2448–2455.
- (61) A. Natan, L. Kronik, H. Haick, R. Tung, *Adv. Mater.* **2007**, *19*, 4103–4117.
- (62) G. Heimel, F. Rissner, E. Zojer, *Adv. Mater.* **2010**, *22*, 2494–2513.
- (63) B. Kretz, D. A. Egger, E. Zojer, *Adv. Sci.* **2015**, *2*, 1400016.
- (64) S. V. Aradhya, J. S. Meisner, M. Krikorian, S. Ahn, R. Parameswaran, M. L. Steigerwald, C. Nuckolls, L. Venkataraman, *Nano Lett.* **2012**, *12*, 1643–1647.

- (65) J. Xia, B. Capozzi, S. Wei, M. Strange, A. Batra, J. R. Moreno, R. J. Amir, E. Amir, G. C. Solomon, L. Venkataraman, L. M. Campos, *Nano Lett.* **2014**, *14*, 2941–2945.

Graphical TOC Entry



Summary text: Transition voltages respond to the collective action of dipole moments embedded in self-assembled monolayers.